Rev.Adv.Mater.Sci. 15(2007) 56-62

ANALYTICAL METHODOLOGY DEVELOPMENT FOR SILICON-RICH-OXIDE CHEMICAL AND PHYSICAL CHARACTERIZATION

M. Barozzi[1], E. Iacob[1], L. Vanzetti[1], M. Bersani[1], M. Anderle[1], G. Pucker[2] and C. Kompocholis[2]

[1]Physics Chemistry of Surfaces and Interfaces Division, ITC-IRST, Via Sommarive 18, 38050 Trento, Italy
[2]Microtechnologies Laboratory, ITC-IRST, Via Sommarive 18, 38050 Trento, Italy

Received: January 22, 2007

Abstract. Silicon-rich-oxide (SRO) layers and silicon nano-crystals (Si-nc) have been gaining particular attention for their optoelectronic properties. Analytical techniques as secondary ion mass spectrometry (SIMS), photo-electron spectroscopy (XPS), variable angle spectroscopy ellipsometry (VASE) and atomic force microscopy (AFM) were considered in this work as helpful ways to obtain the required characterization of these materials. SRO different films were deposited on Si wafers by plasma enhanced chemical vapor deposition (PECVD) and varying the ratio between SiH_4, N_2O and NH_3. Then they were analyzed by SIMS and XPS, which combine the chemical physical analytical techniques requested to provide quantitative and accurate results. Besides the high precision of SIMS profiles, the accuracy of the data in SRO is marked as a difficult task, because of different matrices in different films. Therefore a fit equation for silicon SIMS depth profiles quantification in SRO is proposed. The physic-chemical data were related to VASE measurements. Furthermore the structural properties of silicon nano-crystals were investigated by AFM. The developed methodology confirms undoubtedly the Si-nc growth.

1. INTRODUCTION

Since 1990 visible light emission from porous silicon were discovered [1] and silicon nano-crystals embedded in various matrices were pointed out as promising materials for new applications in microelectronic. In fact their photoluminescence (PL) properties, related to quantum size effects, are applicable to new lasers, new non-volatile memories and electro-optical devices. These materials have the advantage to be compatible with the actual fabrication processes in microelectronic industry [2]. Si nano-crystals in silicon oxide can be obtained either by Si implantation into SiO_2 matrix, by sputtering, SRO layer chemical vapour deposition, or by SiO_x/SiO_2 multilayer structures deposition [3]; in every case Si clusters or Si-nc grow as precipitates, by annealing the Si supersaturated solid solution at temperatures around 1000 °C. Local Si concentrations in excess of $3 \cdot 10^{21}$ atoms/cm^3 are required for Si-nc formation [4]. The Si mesoscopic particles size, obtainable trough these processes, tends to increase as the Si concentration and the annealing temperatures increase [5]. As alternative method monodispersed Si nano-crystals are also obtained by using VHF plasma enhanced decomposition of silane gas, with a precise control of nucleation for Si-nc dimensions and growth period [6].

Corresponding author: M. Barozzi, e-mail: barozzi@itc.it

© 2007 Advanced Study Center Co. Ltd.

Accurate and precise analytical techniques for materials characterization are requested to obtain a detailed correlation of SRO and Si-nc growth processes with their optoelectronic properties. The samples analyzed in the present work for an analytical methodology development are Si-nc based MOS-LED. Chemical-physical-optical and structural techniques are here considered and discussed for silicon characterization in SRO films.

SIMS is a very sensitive and precise technique for element quantification, but it requires reference standards to obtain a good accuracy on elements concentration. In fact the ion yield of the interesting elements varies with the sputtered matrix (i.e. matrix effects) and the analytical conditions. Assuming constant and stable analytical conditions [7], a relative sensitivity factor RSF is usually calculated on measured standards to convert secondary ion signals in atomic concentrations [8]. The accuracy for elements concentration in the target samples and in the standard is the same, until the matrix is unchanged and the elements are in dilute regime. Unfortunately this is not the SRO case, where the matrices compositions differ deeply with the various growth processes. Therefore SIMS quantification of elements in SRO with variable concentration of oxygen, silicon and nitrogen is not trivial.

VASE is commonly used to measure thickness and dielectrical functions of single layer and multi-layered materials [9]. VASE is a very accurate method - for this purpose -for films of homogeneous composition and materials such as SiO_2, Si_3N_4, SiON. Often ellipsometric spectra are also analysed using an effective medium approximation to predict the optical constants of mixtures obtained from materials of known optical constants. This approach allows obtaining information on the sample composition, but suffers the fact that the microstructure and bonding properties can not very easily be described by the simple mixture of a certain number of components. It is therefore interesting to check the reliability of the results from VASE analysis by comparing them with the ones obtained from other techniques, as SIMS and XPS.

AFM provides very useful morphological information, which can confirm the growth of Si-nc embedded in SRO films. An etching method of SRO in fluoridric acid solution HF is here successfully applied to reveal the nano-crystals.

2. EXPERIMENTAL

The SRO films were obtained by PECVD, with different composition, on p-type <100> silicon wafers. The wafers were cleaned before deposition by using a RCA wet cleaning process [10]. The composition of the films is commonly defined by the ratio of N_2O to SiH_4, called Γ. Lower Γ means higher excess of silicon with respect to stoichiometric SiO_2. In addition films of this kind deposited by PECVD may contain some nitrogen. In two of the samples NH_3 was added during the deposition process, with the intention of changing the nitrogen content and to evaluate its impact. After SRO three additional layers were deposited, consisting of approximately 15nm of in situ phosphor doped poly-Si and 30 nm Si_3N_4 (by LPCVD), plus 100 nm SiO_2. These capping layers are used as diffusion barrier during wet oxidation process. Wet oxidation, accomplished at 1050 °C for 1 hour, is required for both device isolation and decomposition of SRO in SiO_2 and Si-nc. Finally both the SiO_2 and Si_3N_4 layers were removed by dedicated wet-etching processes. For the XPS analysis also the poly-Si layer had to be removed. For this purpose we used a wet-etching process with poly-etch (HF -HNO_3-H_2O). The etch time was calculated to remove the poly-Si layer of 20nm (over-etching 25%).

XPS measurements were performed using a Gammadata Scienta Esca-200 system equipped with a monochromatized Al K_α (1486.6 eV) source. An overall energy resolution of 0.4 eV is routinely used. All the measurements were performed at a fixed emission angle of 90°. In these experimental conditions the sampling depth is approximately 10 nm. For each sample, Si 2p, O 1s, N 1s, and C 1s core levels were collected. All core level peak energies were referenced to the saturated hydrocarbon in C 1s at 285.0 eV.

SIMS analyses were performed by a Cameca SC-ultra magnetic sector apparatus. MCs^+ analytical methodology has been used, in order to reduce as much as possible the matrix effects on SIMS profiles [11,12]. In this method the monitored secondary species are positive molecular ions MCs^+ combining the re-sputtered primary ions Cs^+ with M atomic species sputtered from the sample surface. Cs^+ at 1keV impact energy was used as primary sputtering beam and $^{133}Cs^+$, $^{28}SiCs^+$ were monitored. An electron beam for electric charge compensation was applied during the sputtering process.

The depth scale was calibrated for each sample by measuring the crater depth at the SRO/Si sub-

strate interface, by a Tencor P15 mechanical profilometer.

VASE spectra of the samples were measured with a Jobin Yvon UVISEL 460 AGAS/RS ellipsometer in the wavelength range 400 to 1300 nm at incidence angles of 50°, 60°, and 70° degree after the removal of the Si_3N_4 and SiO_2 layer.

AFM images on sample Γ3 were acquired by a NT-MDT Unisolver Scanning Probe Microscope. The Si nano-crystals embedded in SRO layer were exposed to samples surface by wet etching the samples in HF 1% for 10 seconds. The wet etching removes preferentially the silicon oxide therefore Si-nc structures are revealed. The AFM analyses were performed in semi-contact mode by using a silicon tip (~ 10 N/m, ~ 250 KHz) with a nominal radius less than 10nm.

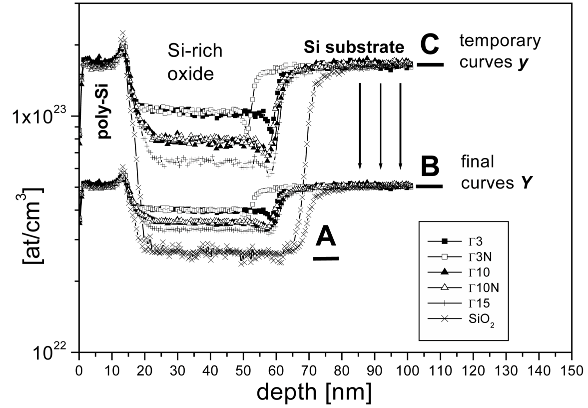

Fig. 1. Silicon SIMS depth profiles of poly-Si / Si rich oxide / Si substrate, before (curves *y*) and after (curves *Y*) linear fit between the Si concentrations in SiO_2 and Si bulk. Γ defines the N_2O to SiH_4 ratio during SRO deposition.

3. RESULTS

The SIMS depth profiles on SRO samples with various Γ compositions were normalized point by point to Cs^+ secondary ion signal.

As anticipated it is not possible to use a single RSF for Si quantification, because of matrix effects occurring when the matrices change. Artefacts are generated due to ion yield variations, as can be seen in Fig. 1 (temporary curves *y*). A fitting procedure was used for the calculation of Si atomic concentration in SRO films deposited with various Γ. The stoichiometric SiO_2 film and Si bulk are assumed as fixed bounds for minimum ($A = 2.65 \cdot 10^{22}$ atoms/cm^3) and maximum ($B = 5.06 \cdot 10^{22}$ atoms/cm^3) Si concentrations respectively. A silicon dioxide film SiO_2 was used for reference.

The next points are followed for Si quantification.

1. A scaling factor F is obtained by normalizing the raw SIMS profile measured on sample SiO_2 to the nominal concentration of Si in silicon dioxide (A). Every curve Γ, with variable Si amounts, is then increased for same factor F (in at/cm^3 on counts/s). We name y the new temporary curves.
2. C is the resulting Si concentration in Si bulk, as obtained at point 1, which is a temporary value (Fig. 1). By these analytical conditions C appears overestimated compared to the expected nominal value $B = 5.06 \cdot 10^{22}$ atoms/cm^3)
3. A simple fitting curve to obtain the final SIMS profiles of Si concentrations Y is then applied:

$$Y = \frac{B - A}{C - A} \cdot (y - A) + A.$$

The resulting Γ and SiO_2 curves are collected in Fig. 1. The silicon depletion noted at the SRO/Si-substrate interface is related to the presence of native SiO_2, about 1.5 nm thick, not removed before the SRO deposition. An apparent excess of silicon noted at the poly-Si/SRO interface is instead an artefact not yet understood. For this set of samples and inside the SIMS precision, NH_3 added during the SRO deposition does not change the calculated silicon content.

In the analysis and modeling of the VASE spectra a two layer model was used. In the first step the VASE spectrum of the sample SiO_2 (with poly-Si top layer on silicon dioxide) was used to develop a suitable dielectric function for the optical parameters of the poly-Si layer. We found that a suitable model for the dielectric of the poly-Si layer can be obtained by a combination of the dielectric function of c-Si and an additional oscillator. This additional oscillator accounts mainly for the higher absorption of the phosphor doped poly-Si layer in the wavelength range from 400 to 600 nm. The silicon oxide layer of wafer SiO_2 was modeled with a Cauchy-type function. The thickness of the layers obtained with this model are $d_{poly\text{-}Si} = 12.6 \pm 0.2$ nm for poly-Si film, and $d_{SRO} = 57.3 \pm 0.2$ nm for the SiO_2 layer. The refractive index of the SiO_2 layer at 633 nm n_{633} is 1.485, which is a reasonable value for SiO_2 glasses.

The dielectric function obtained for the poly-Si layer was then used for the analysis of the VASE

Table 1. Gas flow during PECVD film deposition, refractive index at 1200 nm n_{1200}, film thickness by VASE and SIMS. The number within the sample name after the symbol Γ indicates the ratio of N_2O to SiH_4 during deposition.

Sample name	SiH_4 [sccm]	N_2O [sccm]	NH_3 [sccm]	n_{1200} VASE	$d_{poly\text{-}Si+SRO}$ [nm] VASE	$d_{poly\text{-}Si+SRO}$ [nm] SIMS
Γ3	258	778	-	2.494±0.003	59.0±0.2	58.5±4
Γ3N	258	778	100	2.138±0.007	46.3±0.2	52.0±4
Γ10	94	945	-	1.898±0.003	62.1±0.2	60.0±2
Γ10N	94	945	40	1.904±0.003	59.7±0.2	58.5±2
Γ15	65	974	-	1.680±0.003	62.0±0.2	59.5±1
SiO_2	12	1420	*392(N_2)	1.468±0.003	69.9±0.2	68.5±2

Table 2. The Si content in SRO films was calculated by VASE, XPS, and SIMS. SIMS provides only atomic concentrations because the films have various matrices.

Sample name	Si-content at.%, XPS	Si-content at.%, VASE	Si-content [at/cm^3], VASE	Si-content [at/cm^3], SIMS
Γ3	63	66.3	$3.8 \cdot 10^{22}$	$4.0 \cdot 10^{22}$
Γ3N	65.7	66.1	$3.6 \cdot 10^{22}$	$4.0 \cdot 10^{22}$
Γ10	—	51.0	$3.1 \cdot 10^{22}$	$3.5 \cdot 10^{22}$
Γ10N	52.4	50.7	$3.2 \cdot 10^{22}$	$3.6 \cdot 10^{22}$
Γ15	49.1	44.3	$2.9 \cdot 10^{22}$	$3.3 \cdot 10^{22}$
SiO_2	—	33.33	$2.2 \cdot 10^{22}$	$2.65 \cdot 10^{22}$

spectra of all the other samples and all the analysis described in the following lines. The layer thickness of both poly-Si layer and SRO layer was obtained by fitting the VASE spectra in the spectral range 1000 nm to 1300 nm, using a constant refractive index for the SRO layer (in this spectral region the SRO layers can be assumed to have very low absorption and low dispersion). The sum of the thicknesses of both layers (*d*poly-Si + SRO) together with the refractive indices are given in Table 1. With the known layer thickness the VASE spectra were again fitted assuming that the SRO can be represented by a mixture of the dielectric functions of c-Si, SiO_2, and Si_3N_4, mixing them using the Bruggeman equation in effective medium approximation. This method was used by several authors to analyze the ellipsometric spectra of materials with composition similar to our samples [13,14]. From the volumes fractions obtained by this fit, we can calculate the Si, N, and O content assuming that the density is the same as for the bulk materials. This analysis provides the Si-content of the SRO in atomic percentage (see Table 2).

The XPS results for silicon concentration on the measured samples are reported in Table 2. The values (in atomic percentage) were calculated using the atomic sensitivity factors. In Fig. 2 the Si 2p core level spectra are reported for two representative samples. The sample Γ3, with high silicon content, presents a line shape with a well defined doublet at lower binding energy (elemental silicon, or Si(0)), a second peak located at the SiO_2 binding energy (Si(4+)), with a tail in between, indicating the presence of other kind of bonds (i.e. suboxides). The doublet is the evidence of Si crystallization in this sample and it implies Si crystals dimensions bigger than 10 nm. Sample Γ3N (not shown) reveals a similar behaviour. In the Γ15 spectrum, instead, the typical Si(0) peak appears, but it is not well resolved, indicating an amorphous nature of the elemental silicon present in the SRO layer. The dominant peak is the Si(4+) one. In addition, the tail between the two main peaks indicates the pres-

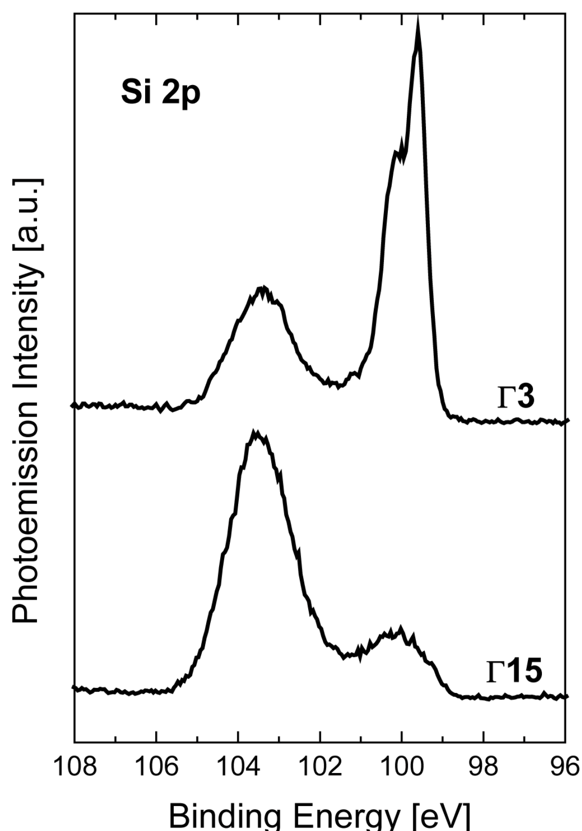

Fig. 2. The Si crystallization in sample Γ3 is evidenced by the doublet peaks at lower binding energy in XPS measurements. In Γ15 the Si chemical state is amorphous.

ence of other bonds (suboxides and nitrides). Similar results were observed for sample Γ10N. There appears to be a threshold in silicon concentration for the formation of nanocrystals. The evaluation of the threshold composition would require an investigation of a larger number of samples.

AFM images on sample Γ3 are reported in Fig. 3. The Si-nc structure and distribution are well defined and confirm the XPS results on the same sample. The crystals diameter is estimated in a range of 16 ÷ 30 nm. Their height is relatively small, between 1 ÷ 5 nm, but it depends mainly on the etching process. The same etching process route repeated on stoichiometric SiO_2 does not generate these structures and the resulting surface roughness is less than 1 nm. Similar results were obtained by other authors for different SRO samples without etching the surface [15], but the advantage of SiO_2 removal is here remarked for a better definition of Si-nc morphology.

4. DISCUSSION

Accurate and precise characterization methodologies are recognized as a keystone to correlate the growth process of these materials and their opto-electronic properties. SIMS analyses are useful for prompt determination of layers thickness. SIMS is also very sensitive to elements and accurate if standards of known composition are used, otherwise approximations and fitting procedure are required. Looking at definition of RSF [8], RSF values for silicon coincide merely with the nominal concentrations *A* of Si in SiO_2 and *B* of Si in Si bulk. Instead SRO films represent intermediate conditions, where RSF are unknown and can not be calculated because Si concentrations and Si ion yield are also variable. Therefore the proposed fitting algorithm is a simple quantification method without RSF but it can also be seen as a fitting between two RSF values, in SiO_2 and Si bulk.

The accuracy of the concentrations has to be verified by using alternative and independent analytical methods, anyway the relative comparison among the samples are meaningful.

The total film thicknesses, measured by a Tencor P15 on the SIMS sputtered craters, were compared to the ones obtained from VASE measurements. The thickness values are given in Table 1 and the agreement between both methods is excellent. The only sample for which the layer thickness shows considerable differences is the sample Γ3N with a thickness of 46.3±0.2 (VASE) and 52±4nm (depth profiling). This sample shows some anomaly behaviour in the VASE analysis. The refractive index is considerably lower than the one of sample Γ3, which is an indication of a considerably lower a-Si or poly-Si content. Although the goodness of the fit for sample Γ3N is similar to the ones of the other samples it can not be excluded that there is a problem with the model used for thickness evaluation for this particular sample. In general both methods give a good estimate of layers thicknesses, while VASE offers the advantage to be a non-destructive technique.

Comparing the Si-content obtained from VASE, XPS, and SIMS (Table 2) one has to consider advantages and disadvantages of every method: the results from VASE depend strongly on the models used in fitting the ellipsometric spectra. The disagreement between Si atomic concentrations provided by SIMS and VASE depends mainly on sample SiO_2. This film, growth as reference sample for the fitting procedure on SIMS profiles, seems not stoichiometric as expected. The mean devia-

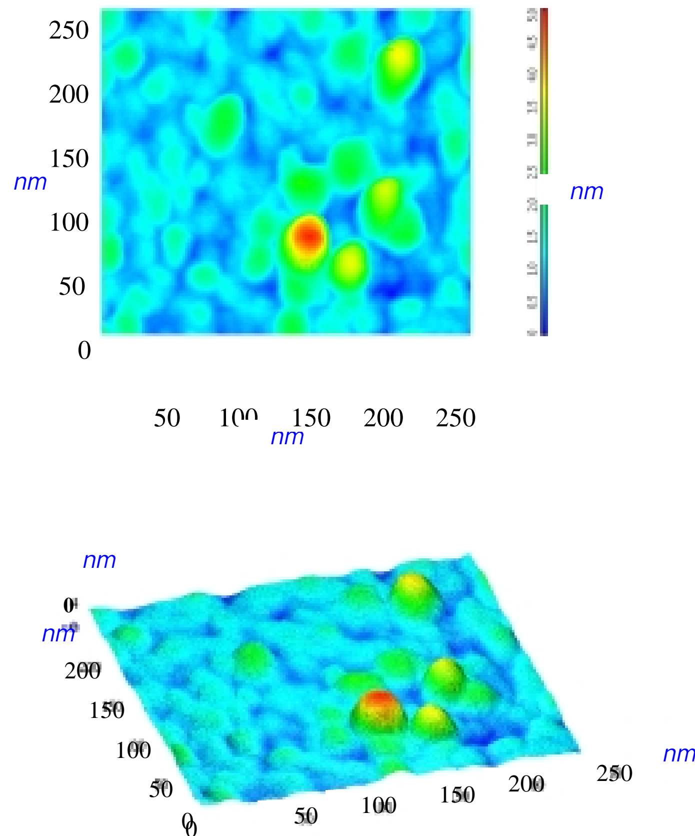

Fig. 3. AFM images confirm the presence of Si nano-crystals embedded in SRO film. The mean size is between 16 ÷ 30nm.

tion of SIMS data from VASE can be reduced from 13% to 6% by adjusting the fitting curve *Y* with a new reference value for silicon concentration $A = 2.2 \cdot 10^{22}$ atoms/cm^3. This correction is consistent with the algorithm used for SIMS data processing and provides a good agreement of the results.

XPS, while generally very accurate for samples with a homogeneous depth profile, suffers possible changes in film composition due to the sample preparation process. Anyway remarkable differences among the samples are detected and are coherent with the growth of Si-nc. The chemical characterization provided by XPS measurements confirms the Si nano-crystals formation in SRO with higher excess of silicon, whereas silicon remains in amorphous state in SRO with higher Γ.

AFM offers the advantage of three-dimensional mapping of the silicon particles embedded in the film. The effectiveness of etching method is confirmed and can be implemented to study the Si-nc size and distribution through the layers depth, by changing the dipping time. In this way the correlation of the growth processes with physic-chemical and electro-optical properties of the SRO films will be improved. The minimal crystal sizes detectable in SRO by AFM depend also on the tip radius, because the dimensions of Si-nc and tip have convoluted effects on AFM images. The detectable sizes can be reduced by using even smaller tips.

5. CONCLUSIONS

In this work SIMS, XPS, VASE, and AFM are discussed as useful analytical techniques for the physic-chemical and structural characterization of SRO films. This methodology reveals undoubtedly the Si-nc growth in films with higher excess of silicon. A larger number of Si-nc based MOS-LED will be considered in order to improve the correlation of various techniques, in particular to optimize the fitting models for SIMS and VASE. Detailed analyses about the role of nitrogen, as Si-nc dopant and for its impact on PL properties, are in progress.

REFERENCES

[1] L. T. Canham // *Appl. Phys. Lett.* **57** (1990) 1046.

[2] R. J. Walters, P. G. Kik, J. D. Casperson, H. A. Atwater, R. Lindstedt, M. Giorgi and G. Bourianoff // *Applied Physics Letters* **85** (2004) 2622.

[3] M. Perego, M. Fanciulli, C. Bonafos and N. Cherkashin // *Materials Science and Engineering C* **26** (2006) 835.

[4] G. G. Ross, R. Smirani, V. Levitcharsky, Y. Q. Wang, G. Veilleux and R. G. Saint-Jaques // *Nucl. Instr. and Meth. in Phys. Res. B* **230** (2005) 198.

[5] S. Hayashi and K. Yamamoto // *Journal of Luminescence* **70** (1996) 352.

[6] T. Ifuku, M. Otobe, A. Itoh and S. Oda // *Jpn. J. Appl. Phys.* **36** (1997) 4031.

[7] M. Barozzi, D. Giubertoni, M Anderle and M. Bersani // *Applied Surface Science* **231-232 C** (2004) 768.

[8] D. P. Leta and G. H. Morrison // *Anal. Chem.* **52** (1980) 514.

[9] H.G. Tompkins and W. A. McGahan, *Spectroscopic Ellipsometry and Reflectometry – A user's guide* (John Wiley & Sons, New Jork, 1999).

[10] W. Kern and D. Poutinen // *RCA Review* **31** (1970) 187.

[11] M. R. Frost and C. W. Magee // *Appl. Surf. Science* **104/105** (1996) 379.

[12] Y. Gao // *J. Appl. Phys.* **64** (1988) 3760.

[13] A. Szekeres, S. Alexandrova, M. Modreanu, P. Cosmin and M. Gartner // *Vacuum* **61** (2001) 205.

[14] B. Hajji, P. Temple-Boyer, F. Olivič and A. Martinez // *Thin Solid Films* **354** (1999) 9.

[15] M. A. Salem, H. Mizuta, S. Oda, Y. Fu and M. Willander // *Japanese Journal of Appl. Physics* **44** (2005) 88.